Neuron, Vol. 44, 637–650, November 18, 2004, Copyright ©2004 by Cell Press

The AMPA Receptor Subunits GluR-A and GluR-B Reciprocally Modulate Spinal Synaptic Plasticity and Inflammatory Pain

Bettina Hartmann,[1] Seifollah Ahmadi,[2] Paul A. Heppenstall,[3,4] Gary R. Lewin,[4] Claus Schott,[5] Thilo Borchardt,[6] Peter H. Seeburg,[6] Hanns Ulrich Zeilhofer,[2] Rolf Sprengel,[6] and Rohini Kuner[1,*]

[1]Institute for Pharmacology
University of Heidelberg
Im Neuenheimer Feld 366
69120 Heidelberg
Germany

[2]Institute for Experimental und Clinical Pharmacology and Toxicology
University of Erlangen-Nürnberg
Fahrstrasse 17
D91054, Erlangen
Germany

[3]Clinic for Anesthesiology und operative Intensivemedicine
Charité—Universitätsmedizin Berlin
Campus Benjamin Franklin
Hindenburgdamm 30
12200 Berlin
Germany

[4]Max-Delbrück Center for Molecular Medicine
Berlin-Buch
Robert-Rössle-Str. 10
13092 Berlin
Germany

[5]Department of Neonatology
Children's Hospital of the University of Heidelberg
Im Neuenheimer Feld 154
69120 Heidelberg
Germany

[6]Max-Planck Institute for Medical Research
Jahnstrasse 9
69120 Heidelberg
Germany

Summary

Ca^{2+}-permeable AMPA receptors are densely expressed in the spinal dorsal horn, but their functional significance in pain processing is not understood. By disrupting the genes encoding GluR-A or GluR-B, we generated mice exhibiting increased or decreased numbers of Ca^{2+}-permeable AMPA receptors, respectively. Here, we demonstrate that AMPA receptors are critical determinants of nociceptive plasticity and inflammatory pain. A reduction in the number of Ca^{2+}-permeable AMPA receptors and density of AMPA channel currents in spinal neurons of GluR-A-deficient mice is accompanied by a loss of nociceptive plasticity in vitro and a reduction in acute inflammatory hyperalgesia in vivo. In contrast, an increase in spinal Ca^{2+}-permeable AMPA receptors in GluR-B-deficient mice facilitated nociceptive plasticity and enhanced long-lasting inflammatory hyperalgesia. Thus, AMPA receptors are not mere determinants of fast synaptic transmission underlying basal pain sensitivity as previously thought, but are critically involved in activity-dependent changes in synaptic processing of nociceptive inputs.

*Correspondence: rohini.kuner@urz.uni-heidelberg.de

Introduction

Glutamate receptors of the α-amino-3-hydroxy-5-methylisoxazole-4-propionic acid (AMPA) type mediate fast neurotransmission in the central nervous system and are assembled from four subunits: GluR-A-D (GluR1-4, see Seeburg et al., 2001, for review). In contrast to the GluR-A, -C, and -D subunits, GluR-B contains an arginine at a critical position in the pore-forming M2 segment, which is not genetically encoded. Instead this arginine codon is introduced by RNA editing in the GluR-B transcript. Incorporation of GluR-B into heteromeric AMPA receptor strongly reduces the permeability of the receptor channel to Ca^{2+} ions and modifies current rectification and macroscopic channel conductance (Burnashev et al., 1992). Since GluR-B is widely expressed in the central nervous system (CNS; Monyer et al., 1991; Petralia et al., 1997), an overwhelming majority of AMPA receptors in the CNS has low permeability for Ca^{2+}. Only a subset of neurons, predominantly GABAergic interneurons, and glia cells express AMPA receptors with high Ca^{2+} permeability (Monyer et al., 1991; Geiger et al., 1995).

In recent years, AMPA receptors have emerged as key elements of long-lasting changes in the efficacy of central synapses, which are believed to constitute cellular correlates of complex behaviors such as learning and memory (Malinow and Malenka, 2002; Reisel et al., 2002; Zamanillo et al., 1999; Lee et al., 2003), addiction, and reward (Thomas et al., 2001; Sutton et al., 2003). In particular, synaptic activity regulates AMPA receptor function via modulation of ion channel properties of the receptor and its targeting to the postsynaptic membrane. GluR-A and GluR-B serve as key substrates for activity-induced regulation of synaptic transmission via rapid and selective modifications in their phosphorylation status and binding to scaffolding proteins involved in membrane trafficking, which, in turn, determine their synaptic availability and function (Shi et al., 2001; Liu and Cull-Candy, 2000; Malinow and Malenka, 2002; Lee et al., 2003). Thus, the Ca^{2+} permeability and ion conductance properties of synaptic AMPA receptors are not static features of a particular neuron but are modified dynamically by synaptic activity via rapid alterations in GluR-A and GluR-B subunits.

The dorsal horn of the spinal cord shows a high density of Ca^{2+}-permeable AMPA receptors, particularly in the superficial spinal laminae (laminae I and II), where primary afferents carrying nociceptive and thermoreceptive inputs terminate and synapse on spinal second-order neurons (Engelman et al., 1999). Activation of

Ca^{2+}-permeable AMPA receptors in the spinal dorsal horn can strengthen the AMPA receptor-mediated component of synaptic transmission in slice preparations of the spinal cord (Gu et al., 1996). However, very little is currently known about the functional significance of Ca^{2+}-permeable AMPA receptors in spinal processing of nociceptive inputs in vivo. Furthermore, the involvement of Ca^{2+}-permeable AMPA receptors in mechanisms underlying potentiation or sensitization of nociceptive transmission, which are associated with inflammatory and neuropathic pain, has not yet been investigated. Another unusual feature of AMPA receptors in the spinal dorsal horn is their presynaptic localization on terminals of primary afferent sensory nerve fibers (Lu et al., 2002; Lee et al., 2002). Macdermott and colleagues could demonstrate in an elegant set of experiments that activation of presynaptic AMPA receptors inhibits neurotransmitter release at synapses between primary afferents and spinal second-order neurons via primary afferent depolarization, a process which was previously attributed to activation of GABA-A receptors alone (Lee et al., 2002; Engelman and MacDermott, 2004). Thus, AMPA receptors in the spinal dorsal horn demonstrate several striking properties, but the significance of these properties to the spinal gating of nociceptive inputs and behavioral sensitivity to noxious stimuli has yet to be fully explored.

Using mice lacking the genes for GluR-A, GluR-B, or GluR-C, we address here the relevance of AMPA receptor composition in physiological pain and in synaptic plasticity associated with inflammatory pain. We observe that tuning AMPA receptor-mediated synaptic transmission at nociceptive synapses by a differential incorporation of GluR-A and GluR-B reciprocally modulates inflammatory pain-related behaviors. Our findings identify Ca^{2+}-permeable AMPA receptors as key constituents of activity-induced sensitization in pain pathways.

Results

GluR Subunit Distribution and Nociceptive Circuits in GluR-Deficient Mice

In wild-type spinal cord, immunohistochemistry revealed a strong expression of GluR-A in spinal laminae I and II and a weaker and diffuse expression in deeper dorsal horn laminae (Figures 1A and 1B), consistent with previous reports (Brown et al., 2002; Engelman et al., 1999). Although GluR-B immunoreactivity was observed throughout the spinal dorsal horn, labeling was most abundant in inner lamina II and only sparse in outer lamina II (Figures 1A and 1B and data not shown), as described previously (Engelman et al., 1999). The majority of the GluR-A and GluR-B immunoreactivity was found in somata, whereas the spinal neuropil only showed a very weak and diffuse labeling. As expected, spinal cords of *GluR-A*$^{-/-}$ mice and *GluR-B*$^{-/-}$ mice were entirely devoid of GluR-A and GluR-B expression, respectively (Figure 1B). An antibody recognizing both GluR-B and GluR-C demonstrated diffuse labeling of the spinal dorsal horn, which was reduced in intensity in *GluR-B*$^{-/-}$ mice and *GluR-C*$^{-/-}$ mice (data not shown). Although the subcellular distribution of GluR subunits was not studied in detail here, no gross abnormalities were observed in the strengths or patterns of expression in the remaining GluR subunits of GluR-deficient mice (Figure 1B; data not shown). Confocal immunofluorescence of substance P- and isolectin-B_4-positive afferent terminals (Nagy and Hunt, 1982) revealed a grossly normal distribution of terminals of nociceptive and thermoreceptive primary afferents (Figure 1B) in the superficial dorsal horn and a normal distribution of sensory neuron subtypes in the dorsal root ganglia (data not shown) of adult GluR knockout mice.

Striking Changes in Spinal Ca^{2+}-Permeable AMPA Receptors in GluR-Deficient Mice

To determine whether changes in the expression of the GluR subunits in spinal neurons altered the distribution of Ca^{2+}-permeable AMPA receptors in the different laminae of the spinal cord, we analyzed kainate-induced cobalt uptake on live slices of spinal cords derived from GluR-deficient mice and wild-type mice (Figure 2). In initial experiments, spinal sections were colabeled with an anti-substance P antibody or isolectin-B4 to aid in the recognition of the spinal laminae. The pattern of cobalt uptake induced by bath application of kainate (250 μM) in wild-type mice was essentially identical to previous reports (Engelman et al., 1999; Albuquerque et al., 1999). We found a large number of cells positive in laminae I, II, III, and IV (Figure 2A). Lamina II showed the highest density of cobalt-positive cells (Figure 2A, summary in Figure 2C). To assess whether this pattern reflected cobalt uptake selectively through AMPA receptors, we preincubated spinal cord slices with a non-selective non-NMDA glutamate receptor channel blocker, CNQX (50 μM; data not shown) or GYKI 53655 (100 μM), which preferentially blocks AMPA receptors (only 20% blockade of kainate receptor-mediated currents; Wilding and Huettner, 1995). CNQX and GYKI 53655 entirely abolished kainate-induced cobalt uptake in spinal slices, whereas preincubation with an NMDA receptor antagonist, D-APV (100 μM), did not have any effect on kainate-induced cobalt uptake (Figure 2A). A quantitative analysis of at least six independent lumbar spinal slices from each mutant indicated that numbers of cobalt-positive cells in laminae III and IV were not significantly different across *GluR-A*$^{-/-}$, *GluR-C*$^{-/-}$, and wild-type mice (see Figure 2B for examples, Figures 2C and 2D for summary; $p = 0.461$). In contrast, laminae II and I demonstrated major differences across the different genotypes of mice (see Figure 2B for examples). In *GluR-A*$^{-/-}$ mice, the number of cobalt-positive cells in laminae II and I was severely reduced as compared with wild-type littermates ($p < 0.001$ for both; Figures 2B and 2C). In striking contrast, *GluR-B*$^{-/-}$ mice exhibited a large excess of cobalt-positive cells in lamina I, II, and III and IV ($p < 0.001$, 0.007, respectively; Figures 2B and 2D). These results indicate that superficial spinal laminae naturally express a mixture of Ca^{2+}-permeable and Ca^{2+}-impermeable AMPA receptors and that the number of Ca^{2+}-permeable AMPA channels is decreased in the absence of GluR-A and increased in the absence of GluR-B. *GluR-C*$^{-/-}$ mice also demonstrate a significant reduction in the number of cobalt-positive cells in spinal lamina I ($p = 0.023$) as well as in lamina II ($p = 0.035$) (Figures 2B and 2C), suggesting that GluR-C also contributes to the formation of Ca^{2+}-permeable AMPA re-

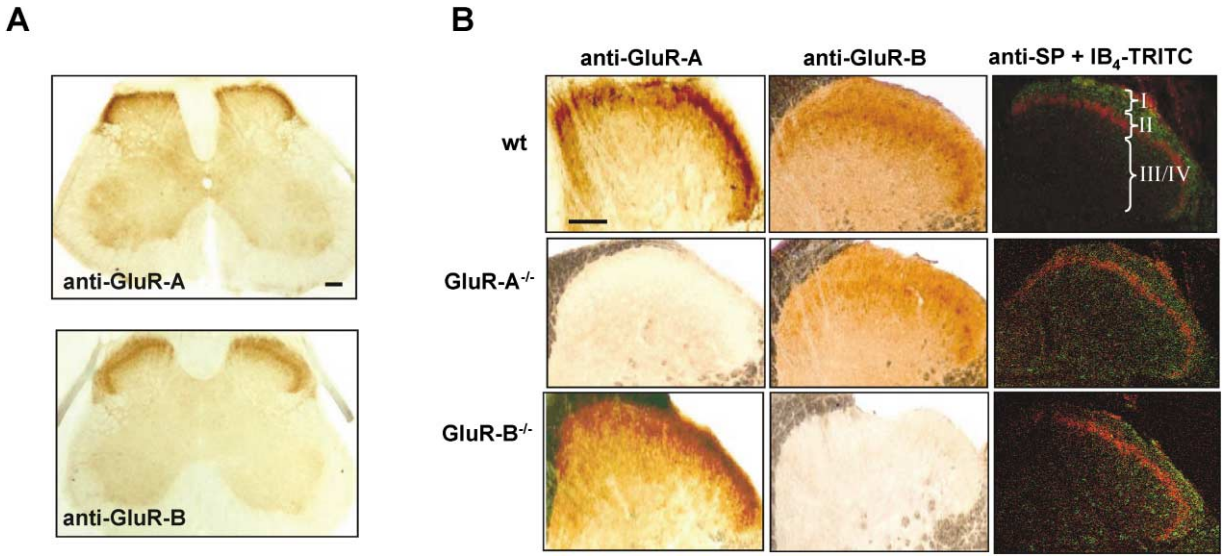

Figure 1. Immunohistochemical Analysis of the Spinal Cords of Wild-Type, GluR-A-Deficient, and GluR-B-Deficient Mice

(A) anti-GluR-A and anti-GluR-B immunoreactivity in the spinal cord of wild-type mice. (B) Immunolabeling of spinal dorsal horns of wt, *GluR-A*$^{-/-}$, and *GluR-B*$^{-/-}$ mice with antibodies recognizing GluR-A, GluR-B, or substance P (peptidergic terminals, green) and staining of isolectin-B4-positive primary nociceptive afferent terminals (red). I–IV indicates spinal laminae I–IV. Scale bars represent 100 μm in all panels.

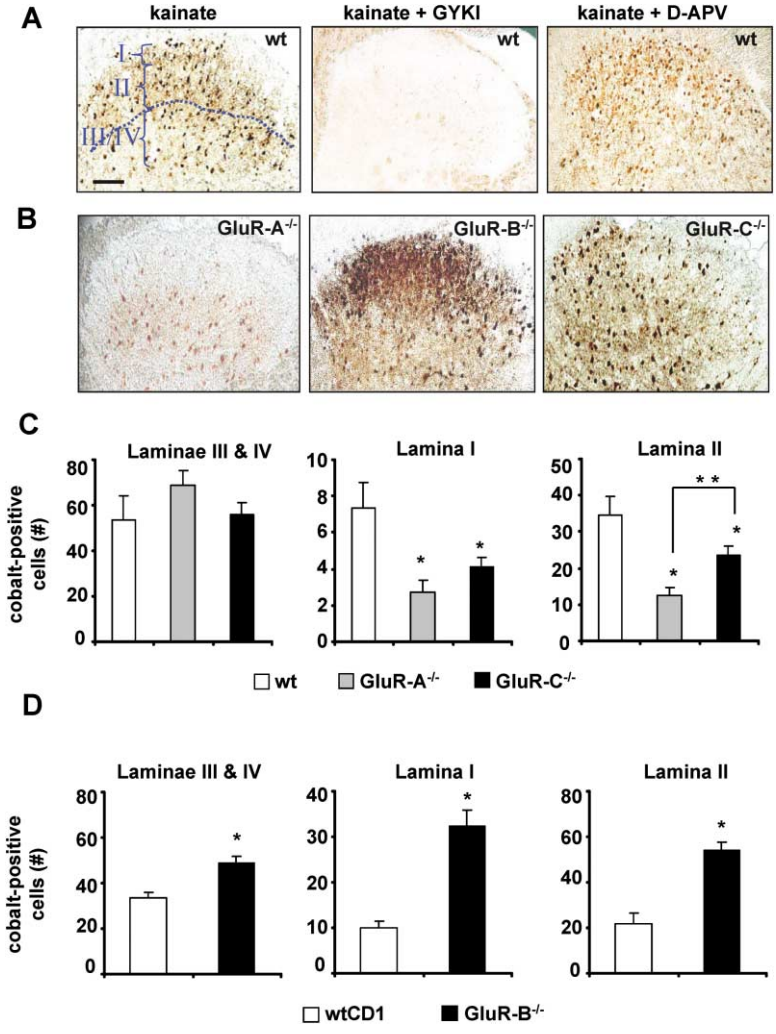

Figure 2. Identification of Ca^{2+}-Permeable AMPA Receptors in Spinal Dorsal Horn of Wild-Type and GluR-Deficient Mice

(A) Representative examples of cobalt uptake induced by kainate (250 μm) in the absence or presence of the AMPA receptor antagonist GYKI (100 μm) or D-APV (100 μm) in C57BL6 wild-type mice (wt). Dotted line in panel (A) is an arbitrary line delineating the superficial spinal laminae (I and II) from deeper spinal dorsal horn laminae, which was drawn based upon colabeling of sections with marker proteins for spinal laminae (data not shown). (B) Representative examples of cobalt uptake induced by kainate (250 μm) in the presence of D-APV (100 μm) in GluR-A-deficient (*GluR-A*$^{-/-}$), GluR-C-deficient (*GluR-C*$^{-/-}$), and GluR-B-deficient (*GluR-B*$^{-/-}$) mice.

(C and D) Quantification of cells demonstrating cobalt uptake in the spinal dorsal horn laminae (I–IV) of *GluR-A*$^{-/-}$ and *GluR-C*$^{-/-}$ mice their wild-type littermates of the C57BL6 stain (wt in [C]) and of *GluR-B*$^{-/-}$ mice and their wild-type littermates of the CD1 strain (wtCD1 in [D]). * and ** indicate statistically significant differences ($p < 0.05$, ANOVA and post hoc Fisher's test) with respect to wild-type and *GluR-A*$^{-/-}$ mice, respectively. Scale bars represent 100 μm in panels (A) and (B). $n = 5–6$ slices per genotype.

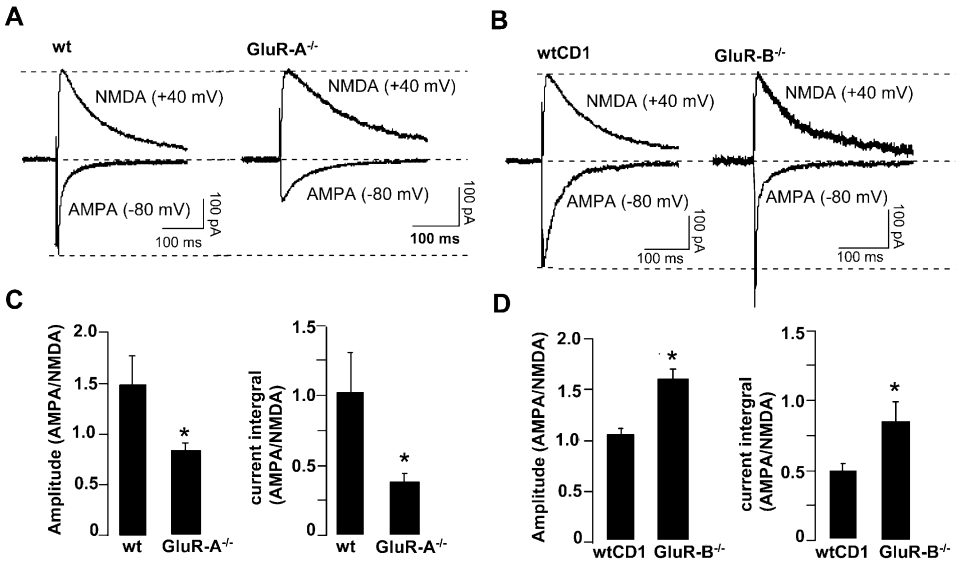

Figure 3. AMPA and NMDA Receptor-Mediated Postsynaptic Current Responses Recorded from Superficial Spinal Dorsal Horn Neurons

(A and B) Averages of ten consecutive current responses recorded at −80 mV (AMPA) or at +40 mV and in the presence of NBQX (NMDA) from GluR-A knock-out mice (*GluR-A*$^{-/-}$) and their wild-type littermates (wt; both genoytpes from the C57BL6 strain, panel [A]) or in GluR-B knockout (*GluR-B*$^{-/-}$) mice and their wild-type littermates (wtCD1, panel [B]). (C and D) Average ratios (mean ± SEM) of AMPA- and NMDA-mediated EPSC amplitudes (left panels) and current integrals (right panels). *p ≤ 0.05 (Student's t test), n = 12–15 neurons for each genotype.

ceptors in spinal laminae that process pain inputs. However, the reduction of spinal cobalt uptake in *GluR-C*$^{-/-}$ mice was significantly less than that in *GluR-A*$^{-/-}$ mice in lamina II ($p = 0.02$).

GluR-A and GluR-B Differentially Modulate Spinal AMPA Channel Currents

To determine how the activation properties of AMPA receptors vary in spinal dorsal horn neurons of GluR-deficient mice, we recorded synaptic currents from visually identified neurons in lamina II of the spinal dorsal horn. The AMPA receptor component of the synaptic currents was recorded at a membrane potential of −80 mV. The NMDA receptor component was pharmacologically isolated using NBQX and recorded at +40 mV (Figures 3Aa and 3Ba). To compensate for inherent variability in the amplitude of synaptically evoked currents across different neurons and slice preparations, the amplitude of AMPA channel-mediated peak current was normalized to the NMDA channel-mediated peak current for each neuron studied (Figures 3A and 3B). The AMPA/NMDA peak current ratio was significantly reduced in spinal neurons derived from *GluR-A*$^{-/-}$ mice as compared to their wild-type littermates (see Figure 3A for example and Figure 3C for summary, $p < 0.05$). In striking contrast, spinal neurons of *GluR-B*$^{-/-}$ mice showed an increased mean AMPA/NMDA current ratio as compared to wild-type littermates (see Figures 3B and 3D; $p < 0.05$). Thus, AMPA channel-mediated peak currents on second-order spinal neurons were significantly reduced in *GluR-A*$^{-/-}$ mice, but significantly enhanced in *GluR-B*$^{-/-}$ mice. The total charge transfer determines the magnitude of postsynaptic depolarization evoked by AMPA receptor activation, which, in turn, is a function of the magnitude of peak currents and the kinetics of current decay. Therefore, to estimate the total charge transfer via AMPA receptors during synaptic transmission in the spinal dorsal horn of mice lacking GluR-A or GluR-B, we analyzed the integral of AMPA and NMDA receptor-mediated synaptic currents in each spinal neuron studied. In comparison with respective wild-type littermates, the mean AMPA/NMDA current integral ratio was decreased in *GluR-A*$^{-/-}$ mice ($p < 0.05$) and increased in *GluR-B*$^{-/-}$ mice ($p < 0.05$).

Intact Basal Neurotransmission and Wind-Up in Spinal Circuits of GluR-Deficient Mice

Postsynaptic AMPA receptors on spinal neurons mediate basal neurotransmission of nociceptive as well as non-nociceptive sensory inputs from primary afferent fibers (Davies and Watkins, 1983). Therefore, we addressed whether changes in the Ca^{2+} permeability and current conductance profiles of spinal AMPA receptors modulate the spinal transmission of primary afferent inputs in GluR-deficient mice by recording ventral root potentials (VRPs) in hemisected preparations of spinal cords (Heppenstall and Lewin, 2001). VRPs evoked by stimulation of dorsal roots at A-δ-fiber or C-fiber stimulation intensities remained unchanged in both *GluR-A*$^{-/-}$ ($p = 0.929$ and 0.421, respectively) and *GluR-B*$^{-/-}$ mice ($p = 0.298$ and 0.973, respectively) in comparison with their respective wild-type littermates (Figures 4A and 4B for examples and Figure 4E for summary).

Moreover, the "wind-up" of VRPs (Heppenstall and Lewin, 2001) remained unaltered in GluR-A and GluR-B knockout mice (Figures 4C–4F), indicating that changes in AMPA receptor properties do not critically influence the rapid summation of postsynaptic responses to repetitive C-fiber inputs.

Reciprocal Changes in Spinal Activity-Induced ERK1/2 Phosphorylation by GluR-A and GluR-B

To investigate the relevance of AMPA receptor composition for activity-dependent changes in nociceptive pro-

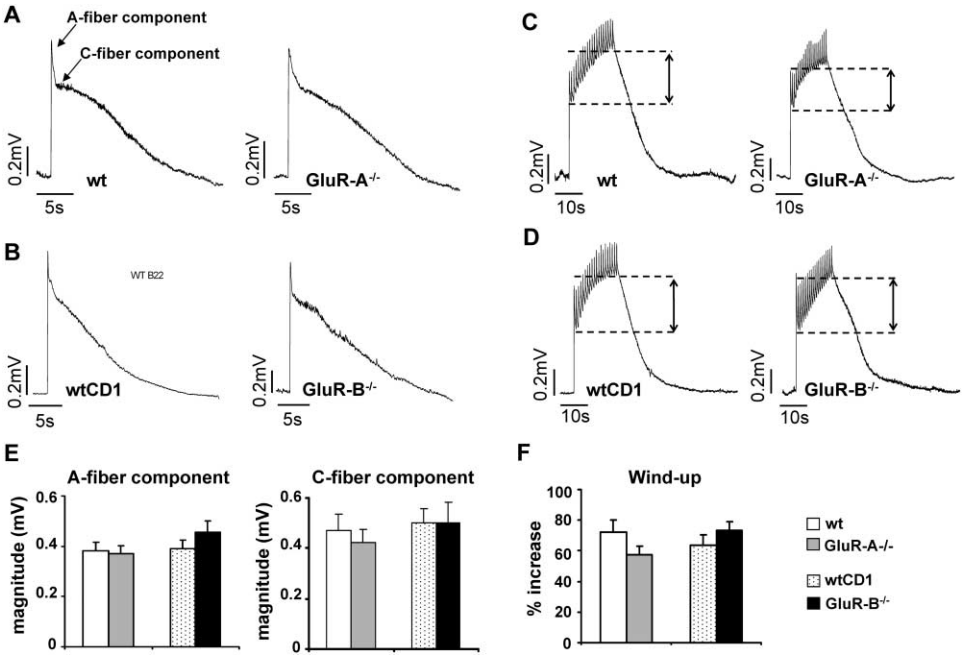

Figure 4. Spinal Transmission in GluR-Deficient and Wild-Type Mice as Estimated by Recording VRPs and Wind-Up of VRPs in Hemisected Spinal Cord Preparations

(A and B) Representative traces of VRPs in GluR-A-deficient mice (*GluR-A*$^{-/-}$) and their C57BL6 wild-type littermates (wt) and in GluR-B-deficient mice (*GluR-B*$^{-/-}$) and their CD1 wild-type littermates (wtCD1). (C and D) Representative traces of wind-up of VRPs in GluR-deficient mice and their wild-type littermates following repetitive C-fiber stimulation are shown. (E) Summary of mean amplitude in millivolts (mV) of the A-fiber-mediated component and C-fiber-mediated component of the VRPs. (F) Summary of VRP wind-up in GluR-deficient mice and their wild-type littermates. n = 6–14 mice per genotype.

cessing in individual spinal laminae, we determined activity-induced phosphorylation of the extracellular receptor-activated MAP Kinases 1/2 (ERK1/2) in spinal cords of GluR mutant and wild-type mice. ERK1/2 are implicated in synaptic plasticity in the hippocampus (Thomas and Huganir, 2004) and are known to be selectively activated in the spinal dorsal horn by peripheral nociceptive input and contribute to inflammatory pain hypersensitivity (Ji et al., 2002). Therefore, we asked whether phosphorylation of ERK1/2 could be used as a spatial readout of plasticity in spinal neurons in response to frequency-dependent stimulation of primary afferent fibers in a slice preparation of the spinal cord with attached dorsal roots. In spinal slices derived from wild-type mice, we found that high-frequency (100 Hz) stimulation of dorsal roots at C-fiber intensity led to an increased phosphorylation of ERK1/2 selectively in the soma and neuropil of spinal lamina I ($p = 0.001$), whereas the deeper laminae did not show any increase in ERK1/2 phosphorylation ($p = 0.656$) (see Figure 5A for examples and Figure 5B for summary of densitometric analysis of phospho-ERK immunoreactivity). Low-frequency C-fiber intensity stimulation (1 Hz) did not alter phosphorylation of ERK1/2 in lamina I ($p = 0.667$; Figures 5A and 5B). Moreover, activity-induced phosphorylation of ERK1/2 was only observed for maximally up to 180 μm in spinal segments along the rostrocaudal axis from the point of entry of the stimulated dorsal root into the spinal cord (the average value was derived from six slices; an example is shown in Figure 5C). These observations indicate that ERK1/2 phosphorylation is a selective and reliable marker for spatially resolving postsynaptic responses in spinal neurons to high-frequency C-fiber inputs. In striking contrast to wild-type littermates, *GluR-A*$^{-/-}$ mice failed to demonstrate ERK phosphorylation in the superficial laminae of the spinal dorsal horn in response to high-frequency C-fiber stimulation (see Figure 5D for example and Figure 5E for summary of densitometric analysis of phospho-ERK immunoreactivity, $p = 0.707$). On the other hand, *GluR-B*$^{-/-}$ mice demonstrated significant phosphorylation following high-frequency C-fiber stimulation (Figures 5D and 5E; $p = 0.018$). These differences in phosphorylated ERK1/2 did not arise from variations in basal expression of ERK1 and -2 across genotypes (Figure 5E; $p > 0.05$ as compared to wild-type mice in all cases). Thus, GluR-A-containing AMPA receptors are required for this paradigm of activity-induced plasticity in the superficial nociceptive laminae of the spinal cord.

Functional Significance of GluR Subunits in Basal and Inflammatory Pain In Vivo

To address the significance of these changes in AMPA receptor properties and activity-induced plasticity in the context of nociceptive processing in vivo, we analyzed behavioral responses to noxious stimuli. When we looked at the latency of the spinal nociceptive tail flick reflex in response to noxious heat (Kolhekar et al., 1993), all mutant mice were indistinguishable from their wild-type littermates (Supplemental Figure S1A [http://www.neuron.org/cgi/content/full/44/4/637/DC1/]), thereby verifying our in vitro observations that basic transmission of nociceptive inputs in the spinal cord is intact in GluR-deficient mice. Similarly, nociceptive reflexes involving activation of higher brain centers, for example,

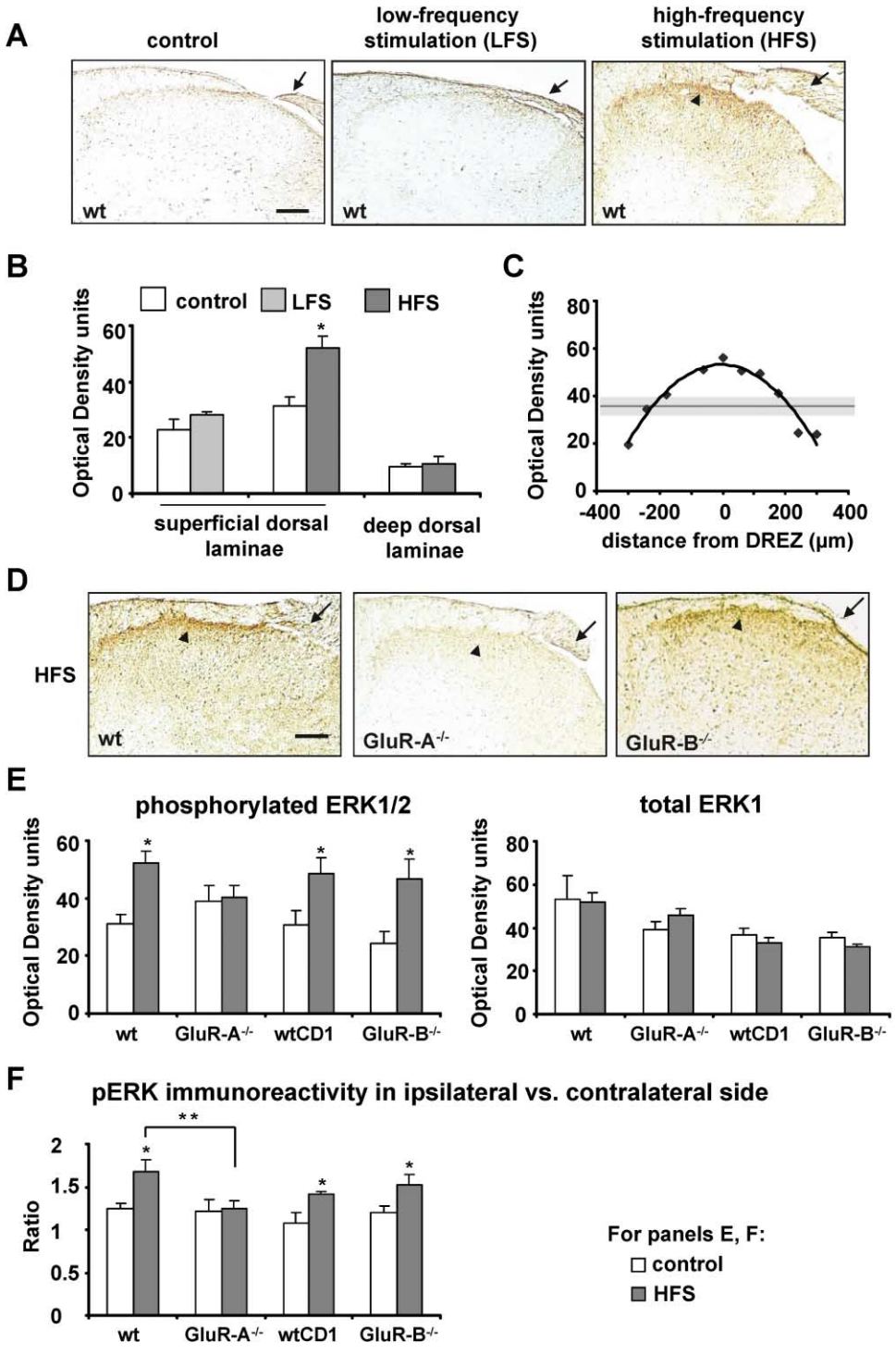

Figure 5. Immunohistochemical Estimation of ERK1/2 Phosphorylation Induced by Stimulation of Dorsal Roots in Spinal Cord Slices Derived from GluR-Deficient Mice and Their Wild-Type Littermates

In panels (B), (C), and (E), the staining intensity in the selected spinal laminae is depicted in units of "optical density" after subtracting background staining values derived from unstained regions in the ventral horn in each individual slice. (A) Typical examples of immunoreactivity for phosphorylated ERK1/2 in the superficial laminae (arrowheads) of spinal slices at 30 min following electrical stimulation of the ipsilateral dorsal root (arrows) at a low frequency (1 Hz, LFS) or high frequency (100 Hz, HFS) or mock treatment (control) in C57BL6 wild-type mice (wt). (B) Densitometric estimation of phospho-ERK1/2 immunoreactivity in superficial spinal laminae and deep dorsal horn following LFS or HFS in wt mice ($n = 9$) (C) An example showing the intensity of phospho-ERK1/2 immunoreactivity in the superficial spinal laminae (fitted to a Gaussian polynomial curve) as a function of distance along spinal segments (in microns) from the point of entry of the stimulated dorsal root (0 μm, dorsal root entry zone [DREZ]) in a wt spinal slice following HFS. Horizontal solid line and gray areas indicate the average and SEM, respectively, of staining intensity in control (unstimulated) slices. (D) Typical examples of immunoreactivity for phosphorylated ERK1/2

hindpaw withdrawal in response to thermal or mechanical stimuli (Hargreaves et al., 1988), remained unchanged in GluR-deficient mice (Supplemental Figure S1B). Thus, neither alterations in Ca^{2+} permeability nor changes in activation properties of AMPA receptors significantly affected basal behavioral responses to nociceptive stimuli. We then tested the extent of sensitization of responses to thermal and mechanical stimuli in GluR-deficient mice in a model of chronic inflammatory pain involving unilateral hindpaw inflammation produced by intraplantar injection of complete Freund's adjuvant (CFA; Hargreaves et al., 1988). The magnitude of paw edema was comparable across mice of all genotypes at 24 hr and 48 hr following unilateral CFA injection (Supplemental Figure S2; $p > 0.05$ for all genoytpes). When tested 24 hr after unilateral CFA injection, mice of all genotypes demonstrated significant decreases in the latency to withdraw from noxious heat (thermal hyperalgesia) and in the mechanical pressure threshold for paw withdrawal (mechanical hyperalgesia) in the inflamed paw in comparison with the control, uninjected paw (Figure 6). *GluR-A*$^{-/-}$ mice, *GluR-C*$^{-/-}$ mice, and their respective wild-type littermates developed similar magnitudes of thermal ($p = 0.644$ and 0.686, respectively; Figure 6A) and mechanical hyperalgesia ($p = 0.146$ and 0.946, respectively; Figure 6B). In contrast, *GluR-B*$^{-/-}$ mice were significantly more sensitive to thermal and mechanical stimuli than their wild-type littermates 24 hr but not at 48 hr following the induction of inflammation ($p = 0.021$ and 0.005 at 24 hr after CFA, respectively; Figures 6A and 6B). Thus, a lack of GluR-B but not of GluR-A or GluR-C can lead to changes in long-term behavioral plasticity in pain pathways.

To address how subunit properties of AMPA receptors affect behavioral correlates of rapid sensitization in pain pathways, we performed the plantar formalin test on GluR mutant mice and wild-type controls (Tjolsen et al., 1992; Vaccarino and Melzack, 1992). Intraplantar injection of formalin in rodents evokes nocifensive behaviors such as licking, shaking, and lifting of the injected paw in a biphasic manner. Phase I of the formalin response (i.e., 0–10 min after injection) involves persistent activation and acute sensitization of nociceptors following peripheral release of peptide neuromediators, whereas the phase II response (i.e., 15 min to 1 hr after injection) involves continual activation of nociceptors and, importantly, a sensitization of central synapses via mechanisms which are triggered by repetitive stimulation during the first phase (Vaccarino and Melzack, 1992; Tjolsen et al., 1992; Ji et al., 1999). Interestingly, the delayed nocifensive responses to formalin that are dependent upon sensitization of central synapses were reciprocally modulated in *GluR-A*$^{-/-}$ and *GluR-B*$^{-/-}$ mice. Whereas mice lacking GluR-A show a reduced second phase as compared to their wild-type littermates ($p = 0.028$; Figure 6C), GluR-B-deficient mice demonstrated a significantly higher magnitude of the phase II response than wild-type littermates ($p = 0.03$; Figure 6C). GluR-C mice failed to reveal any significant changes in the duration of phase I or phase II responses to formalin ($p = 0.66$ and 0.406, respectively; Figure 6C). The reciprocal changes in the phase II response of the formalin test in *GluR-A*$^{-/-}$ and *GluR-B*$^{-/-}$ mice support that acute, short-term plasticity at central nociceptive synapses is dependent on AMPA receptors and their composition.

Surprisingly, both *GluR-A*$^{-/-}$ and *GluR-B*$^{-/-}$ mice demonstrated a significantly longer duration of nocifensive behaviors during phase I of the formalin response in comparison with wild-type controls ($p = 0.036$ and 0.009, respectively; Figure 6C). To test whether this effect reflects a loss of tonic inhibition of neurotransmitter release via presynaptic AMPA receptors on nociceptor terminals, which has been reported in vitro (Lee et al., 2002; Engelman and MacDermott, 2004), we performed the capsaicin test in GluR-A and GluR-B knockout mice and their wild-type littermates. Intraplantar hindpaw injection of capsaicin (0.06%) evokes neurogenic inflammation and nocifensive behaviors due to an acute activation of nociceptors (Laird et al., 2001). In accord with the results from phase I of the formalin response (Figure 6C), both GluR-A and GluR-B knockout mice demonstrated significantly increased spontaneous nocifensive responses to intraplantar capsaicin than their wild-type littermates (Figure 6D), suggesting therefore that AMPA receptors containing GluR-A and GluR-B are involved in the tonic inhibition of neurotransmitter release from primary nociceptive neurons in vivo.

GluR Subunits Modulate Nociceptive Plasticity at Multiple Avenues in Pain Pathways

Synaptic plasticity phenomena associated with hyperalgesia and allodynia in pathological pain states are not restricted to the synapse between nociceptive afferents and second-order spinal neurons but are potentially operational in several brain regions that process the sensory and affective components of pain, including the thalamus, somatosensory cortex, anterior cingulate cortex, hippocampus, and the amygdala (Johansen et al., 2001; Vaccarino and Melzack, 1992; Gebhart, 2004; Flor, 2000). GluR-A and GluR-B are expressed in many of these regions as well as in supraspinal centers that modulate nociception via descending pathways, e.g., the periaqueductal gray (PAG; Tolle et al., 1993). We therefore reasoned that changes in AMPA receptor-mediated neurotransmission and synaptic plasticity in one or several of these supraspinal sites could potentially contribute to the alterations in pain-related behaviors observed in mice lacking GluR-A or GluR-B. To obtain an overview

in the dorsal horn following HFS of dorsal roots (arrows) in spinal slices of GluR-A knockout mice (*GluR-A*$^{-/-}$) and their wild-type C57BL6 littermates (wt) or in GluR-B knockout (*GluR-B*$^{-/-}$) mice. (E) Densitometric estimation of HFS-induced phospho-ERK1/2-immunoreactivity and total ERK1 immunoreactivity in the superficial spinal laminae of *GluR-A*$^{-/-}$ mice and their wild-type littermates (wt) and in *GluR-B*$^{-/-}$ mice and wild-type littermates (wtCD1). (F) HFS-induced phospho-ERK1/2 immunoreactivity in wild-type and GluR mutant mice represented as a ratio of staining intensities in the superficial spinal laminae ipsilateral to the stimulated root to the laminae contralateral to the stimulated root. * indicates significant increase over control slices ($p < 0.05$, ANOVA, post-hoc Fisher's test; $n = 6$–9 slices for each group per genotype). Scale bars in panels (A) and (D) represent 100 μm.

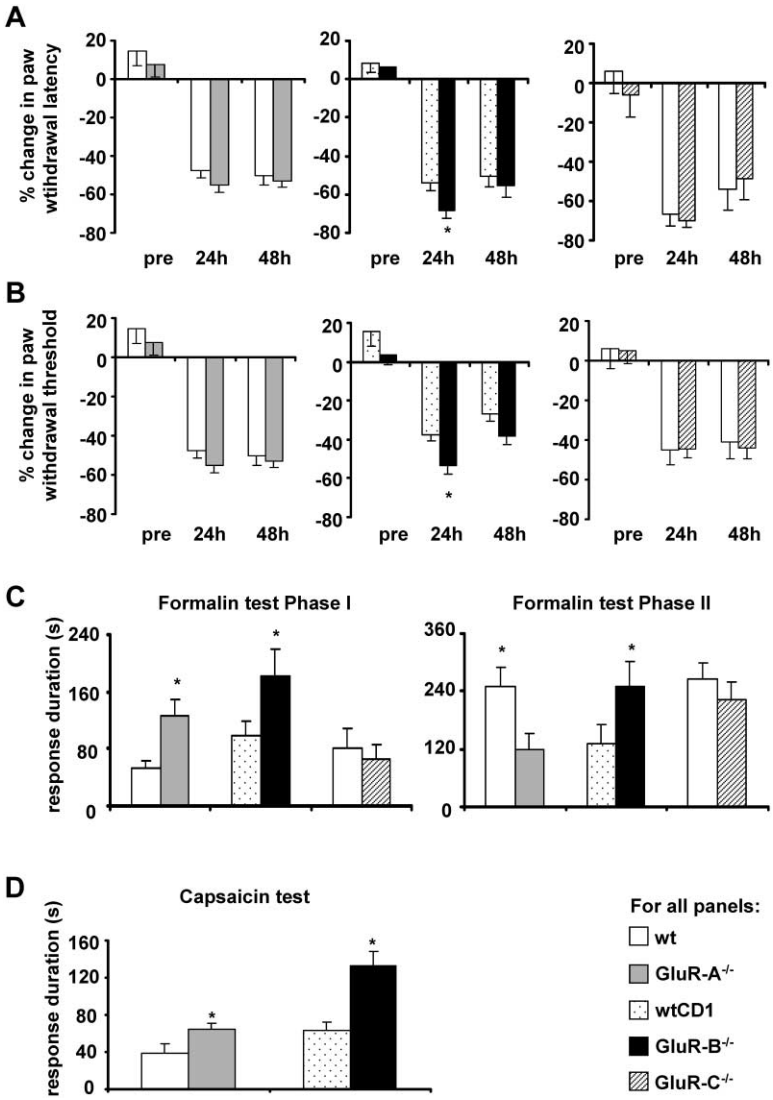

Figure 6. Behavioral Analysis of Postinflammatory Nociceptive Sensitivity in *GluR-A*$^{-/-}$ and *GluR-C*$^{-/-}$ Mice in Comparison with Their C57BL6 Wild-Type Littermates and in GluR-B$^{-/-}$ Mice in Comparison with Their CD1 Wild-Type Littermates

(A and B) Thermal hyperalgesia (changes in latency of paw withdrawal in response to noxious heat [A]) and mechanical hyperalgesia (changes in mechanical threshold [B]), respectively, applied to the hindpaw plantar surface either before (pre) or at 24 or 48 hr (h) following unilateral intraplantar injection of complete Freund's adjuvant (CFA). y axes represent the percent difference in paw withdrawal latency (panel [A], in seconds) or paw withdrawal threshold (panel [B], force in grams) between the injected and uninjected paws calculated as (injected paw − uninjected paw) × 100/uninjected paw (negative values therefore indicate hyperalgesia). (C) Summary of duration of nocifensive behaviors in seconds (s) upon intraplantar injection of 1% formalin during the first 10 min (phase I) and 10–50 min (phase II) of the formalin response. (D) Summary of duration of acute nocifensive behaviors in seconds (s) upon hindpaw intraplantar injection of 0.06% capsaicin. * indicates statistically significant difference as compared to the corresponding wild-type mice. $p < 0.05$, ANOVA, post hoc Fisher's test; n = 10–12 mice per group per test.

of the brain regions that contribute to the hypoalgesia and hyperalgesia observed in GluR-A- and GluR-B-deficient mice, respectively, in the formalin test, we sought a readout that permits a comprehensive comparison of all of the chosen brain regions in every mouse subjected to the formalin test. The immediate early gene c-*fos* is rapidly induced by synaptic activity at multiple avenues in pain pathways in the formalin test and is considered a reliable indicator for the activation status of postsynaptic neurons (Vaccarino and Melzack, 1992; Ma and Woolf, 1996). Hindlimb intraplantar injection of formalin in wild-type mice produced a significant upregulation of Fos in the spinal dorsal horn, the hindlimb somatosensory cortex, the cingulate cortex, limbic structures such as the hippocampus, as well as descending-modulatory centers in the PAG (Figure 7). Fos labeling was very variable in the basolateral and medial amygdala (data not shown). We then compared formalin-induced Fos upregulation in several of these regions in *GluR*$^{-/-}$ mice and wild-type mice. In comparison with wild-type littermates, *GluR-A*$^{-/-}$ mice demonstrated significantly less induction of the Fos gene in the superficial spinal laminae (Figure 7A for examples, Figure 7B for summary, $p = 0.02$). Moreover, in contrast to wild-type littermates, *GluR-A*$^{-/-}$ mice exhibited no Fos induction in the hindlimb somatosensory cortex or cingulate cortex (Figures 7A and 7B; $p = 0.013$ and 0.018, respectively, as compared to wild-type induction), whereas no differences were detectable between wild-type mice and *GluR-A*$^{-/-}$ mice in the hippocampus ($p = 0.306$) and PAG ($p = 0.054$) (Figures 7A and 7B). The reduced Fos staining in the cingulate cortex or hindlimb somatosensory cortex in *GluR-A*$^{-/-}$ mice at 1 hr after formalin injection does not, however, represent a lack of cortical response to acute noxious stimulation, because Fos induction in the cortex of *GluR-A*$^{-/-}$ mice at 30 min after formalin injection was comparable to that seen in wild-type mice (Supplemental Figure S3 [http://www.neuron.org/cgi/content/full/44/4/637/DC1/]). In striking contrast to *GluR-A*$^{-/-}$ mice, *GluR-B*$^{-/-}$ mice exhibited significantly greater Fos induction than their wild-type littermates in the superficial spinal laminae (Figure 8A for examples, Figure 8B for summary, $p = 0.04$). They also showed significant induction of Fos in all brain regions studied,

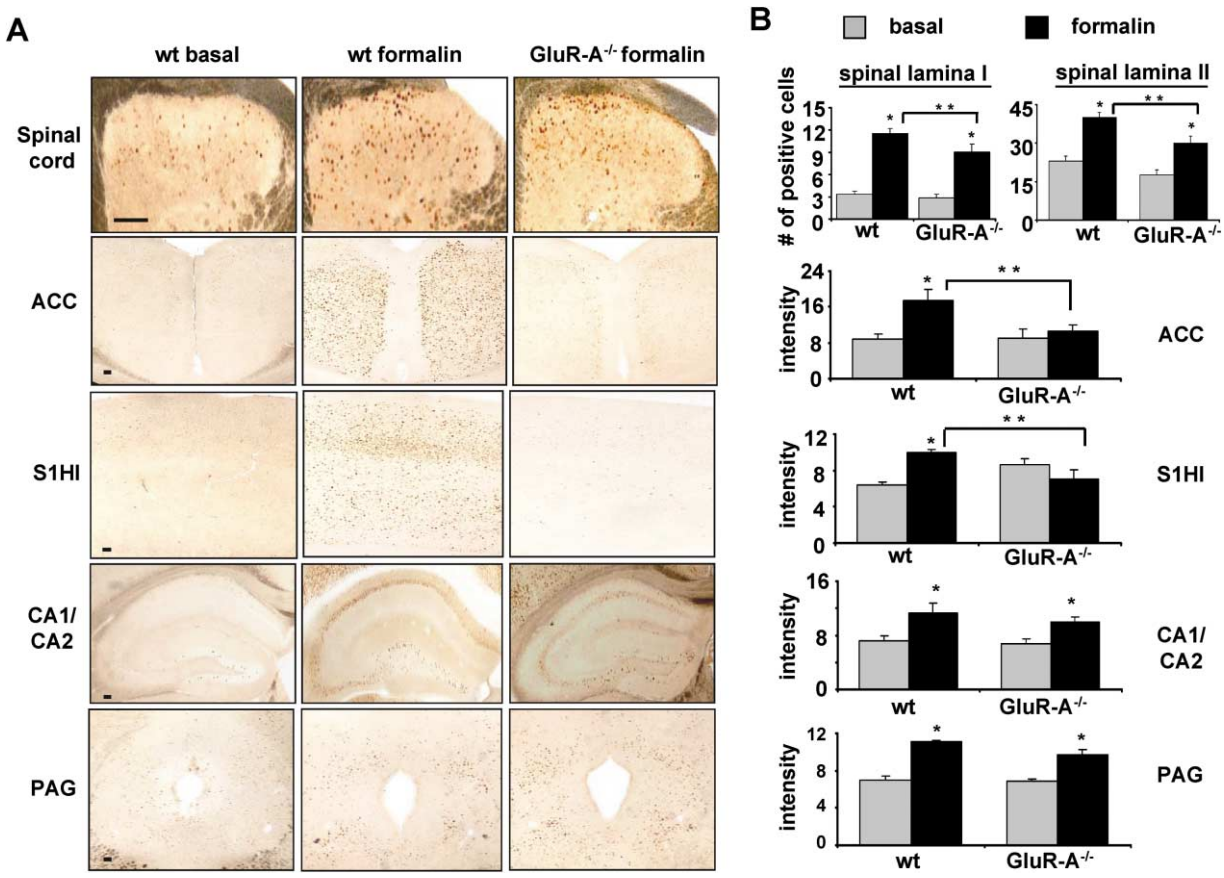

Figure 7. Induction of the c-*fos* Gene in the Pain Pathway in the Formalin Model in Wild-Type Mice and GluR-A-Deficient Mice

Fos immunoreactivity was detected in the spinal dorsal horn, anterior cingulate cortex (ACC), hindlimb somatosensory cortex (S1H1), hippocampal subfields (CA1/CA2), and the periaqueductal gray matter (PAG) at 1 hr following intraplantar injection of 1% formalin in *GluR-A*$^{-/-}$ mice and their wild-type littermates (wt). Typical examples (A) and quantification (B) of either the number of Fos-positive cells (spinal laminae II and I) or the intensity of Fos immunoreactivity (cingulate cortex, S1H1, CA1/CA2, or PAG) in control or formalin-treated mice (induced). * indicates statistically significant differences ($p < 0.05$) between control and induced mice, whereas ** indicates statistically significant differences between induced mice of wt or GluR-A genotypes (ANOVA, post hoc Fisher's test; $n = 3$ mice per genotype). Scale bars in panel (A) represent 100 μm.

but this was not significantly different in magnitude that was observed in wild-type mice ($p > 0.05$ in all cases, Figures 8A and 8B).

Discussion

Cumulative evidence suggests that activity-dependent changes in the efficacy of glutamatergic synapses in pain pathways critically contribute to chronic pain associated with tissue damage or nerve injury (reviewed in Woolf and Salter, 2000; Sandkühler, 2000; Gebhart, 2004). A large number of studies have addressed the role of NMDA receptors and metabotropic glutamate receptors at synapses between primary afferent fibers and spinal neurons and demonstrated that their activation is required for nociceptive hypersensitivity to develop following peripheral tissue injury (Woolf and Salter, 2000). Much less is known about the contribution of spinal AMPA receptors to the pathophysiology of chronic pain. Using a combination of in vitro and in vivo methods, we show here that AMPA receptors in the spinal cord and brain are causally linked to activity-induced nociceptive hypersensitivity.

The spinal cord dorsal horn is unique within the CNS because of its high density of Ca^{2+}-permeable AMPA receptors. We observed that both GluR-A and GluR-C contribute to the formation of Ca^{2+}-permeable AMPA receptors in spinal laminae that process pain inputs. However, the reduction of spinal cobalt uptake in *GluR-C*$^{-/-}$ mice was significantly less than that in *GluR-A*$^{-/-}$ mice in lamina II, suggesting that a majority of Ca^{2+}-permeable AMPA receptors in spinal lamina II are composed either of homomeric GluR-A channels or heteromers of GluR-A with GluR-D. The latter possibility appears less likely because of the very low level of expression of GluR-D in the adult spinal dorsal horn (Tolle et al., 1993; Brown et al., 2002). Because Ca^{2+}-permeable AMPA receptors are expressed on principal neurons as well as on GABA-ergic interneurons in the spinal dorsal horn (Albuquerque et al., 1999), their net contribution to the processing of nociceptive inputs in vivo has remained unpredictable. We observed that *GluR-A* and *GluR-B* knockout mice demonstrated reciprocal changes in the Ca^{2+} permeability of AMPA receptors in spinal laminae receiving nociceptive and thermoreceptive sensory inputs and thus constitute good tools for ad-

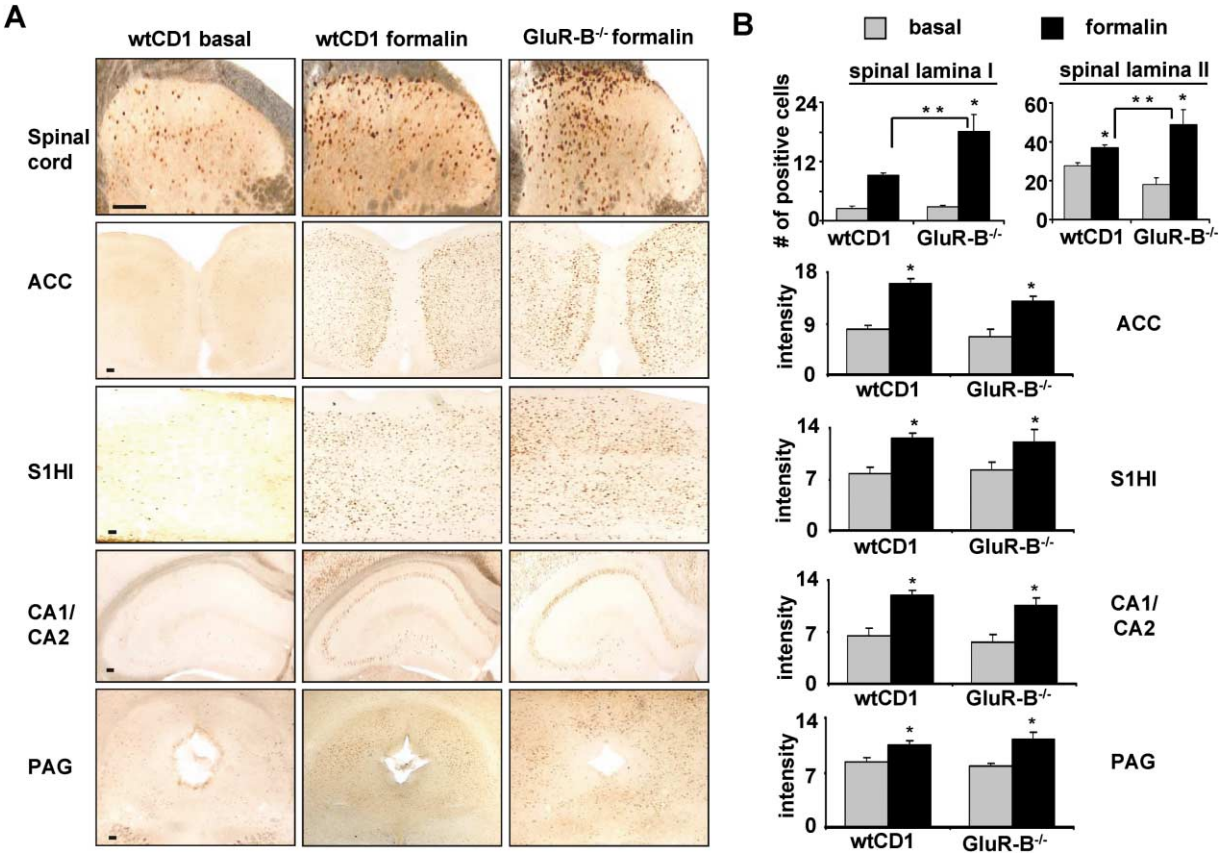

Figure 8. Induction of the c-*fos* Gene in the Pain Pathway in the Formalin Model in Wild-Type Mice and GluR-B-Deficient Mice

Fos immunoreactivity was detected in the spinal dorsal horn, anterior cingulate cortex (ACC), hindlimb somatosensory cortex (S1H1), pyramidal cells in hippocampal subfields (CA1/CA2), and the periaqueductal gray matter (PAG) at 1 hr following intraplantar injection of 1% formalin in GluR-B and their wild-type littermates (wtCD1). Typical examples (A) and quantification (B) of either the number of Fos-positive cells (spinal laminae II and I) or the intensity of Fos immunoreactivity (cingulate cortex, S1H1, CA1/CA2, or PAG) in control or formalin-treated mice (induced). * indicates statistically significant differences between control and induced ($p < 0.05$, ANOVA, post hoc Fisher's test; $n = 3$ mice per genotype). Scale bars in panel (A) represent 100 μm.

dressing the functional significance of Ca^{2+}-permeable AMPA receptors in both nociception and nociceptive plasticity. Because GluR mutant mice demonstrate normal VRPs as well as unaltered behavioral withdrawal responses to noxious stimuli, basal transmission of nociceptive inputs at spinal synapses does not appear to be critically dependent upon subunit properties of AMPA receptors. However, a reduction in AMPA receptor-mediated Ca^{2+} influx and synaptic currents in spinal dorsal horn neurons in GluR-A-deficient mice leads to a loss of acute, short-term nociceptive plasticity in the spinal dorsal horn in in vitro as well as in vivo paradigms. Conversely, an increase in AMPA receptor-mediated Ca^{2+} influx and synaptic currents in the spinal dorsal horn caused by a deletion of GluR-B is associated with an increase in nociceptive activity-induced synaptic plasticity in the spinal dorsal horn in vitro, which is paralleled by an increase in the behavioral manifestations of nociceptive hypersensitivity in vivo. Taken together, these findings show that the composition of AMPA receptors is an important parameter governing excitability and plasticity in nociceptive pathways and suggest that circumstances involving a change in AMPA receptor composition would lead to aberrant processing of nociceptive inputs.

So far, the functional significance of GluR-A and GluR-B in synaptic plasticity has been best studied in the context of long-term potentiation of synaptic transmission in vitro in the hippocampus and the regulation of synaptic strength in paradigms underlying activity-dependent learning in vivo (Takahashi et al., 2003; Jia et al., 1996; Zamanillo et al., 1999; Reisel et al., 2002). Recent evidence suggests that the molecular and cellular mechanisms involved in cognitive and emotional learning are also operational in leaving memory traces in pain pathways, which become manifest as nociceptive hypersensitivity and chronic pain (Ikeda et al., 2003; Sandkühler, 2000; Flor, 2002). Interestingly, analogous to a requirement for GluR-A in hippocampal LTP (Zamanillo et al., 1999), we observe that the GluR-A subunit is required for a rapid sensitization in the spinal dorsal horn. Furthermore, consistent with a role for GluR-A in short-term spatial memory, but not in long-term memory consolidation (Reisel et al., 2002), we observe selective deficits in GluR-A knockout mice in paradigms of early, but not long-lasting, nociceptive hypersensitivity. Con-

versely, GluR-B knockout mice are known to demonstrate enhanced hippocampal LTP (Jia et al., 1996), and we show here that they develop exaggerated sensitization in paradigms of short-term as well as long-term nociceptive hypersensitivity. Thus, our experiments with the GluR mutant mice consolidate the emerging view that sensitization phenomena in the spinal dorsal horn share common molecular mechanisms with hippocampal LTP (Willis, 1997; Sandkühler, 2002).

Furthermore, our data predict that a lack of GluR-B-containing AMPA receptors (or a corresponding enrichment of GluR-A-containing AMPA receptors) would lead to long-lasting nociceptive hypersensitivity in pathological states. When could such circumstances arise and how would they modulate synaptic AMPA receptors? First, peripheral injury could change spinal AMPA receptor composition via transcriptional regulation of GluR genes, as reported in inflammatory pain models (Zhou et al., 2001). Second, along the lines of rapid alterations in the composition of synaptic AMPA receptors induced by activity in the cerebellum (Liu and Cull-Candy, 2000), hippocampus (Shi et al., 2001), and the cortex (Takahashi et al., 2003), persistent activation of primary nociceptive afferent fibers could rapidly regulate synaptic AMPA receptor composition on spinal neurons. This can be achieved by modulating the phosphorylation status of GluR-A and GluR-B subunits and their binding to PDZ domain-containing synaptic scaffolding proteins, thereby changing membrane targeting and synaptic availability of AMPA receptors (Malinow and Malenka, 2002; Takahashi et al., 2003). Interestingly, recent studies report changes in the phosphorylation status of GluR-A in the spinal dorsal horn in postinflammatory states (Fang et al., 2003a, 2003b; Nagy et al., 2004). Furthermore, rapid changes in PDZ domain protein interactions of AMPA receptor subunits in the spinal dorsal horn are associated with serotonin-induced facilitation of spinal synaptic transmission (Li et al., 1999). Third, rapid local dendritic synthesis of GluR subunits could contribute to activity-dependent regulation of AMPA receptor composition at spinal synapses, as demonstrated recently in cultured hipppocampal neurons (Ju et al., 2004). Finally, potential changes in the efficacy of editing of the GluR-B mRNA in disease states could modulate pain pathophysiology by altering AMPA receptor composition in the spinal dorsal horn. Indeed, dysfunctional GluR-B editing has been reported in the spinal cord of humans in neurodegenerative disease states, such as amyotrophic lateral sclerosis (Kawahara et al., 2004), and it remains to be seen whether similar changes occur in patients suffering from chronic inflammatory or neuropathic pain. Thus, it will be very important to direct future studies at these and additional potential molecular mechanisms to fully understand the contribution of spinal AMPA receptors to the development of chronic pain syndromes.

Peripheral injury- or disease-induced alterations in synaptic efficacy occur not only at the first synapse made by the primary nociceptive afferents in the spinal dorsal horn but are also operational in several regions processing the sensorimotor as well as emotional-affective components of pain, such as the thalamus, somatosensory cortex, cingulate cortex, brain stem nuclei, and PAG (Gebhart, 2004; Johansen et al., 2001; Tinazzi et al., 2000) as well as in limbic structures such as the hippocampus (Vaccarino and Melzack, 1992) and amygdala, where AMPA receptor subunits are expressed (Tolle et al., 1993; Geiger et al., 1995; Petralia et al., 1997). Both short-term and long-term plastic changes in cortical glutamatergic synaptic transmission occur in the cortex in animal models of pathological pain (Johansen et al., 2001) and in humans (Flor, 2002). Interestingly, *GluR-A*$^{-/-}$ mice demonstrated a specific reduction in activity-induced Fos upregulation associated with a sensitization of noxious inputs in the hindlimb somatosensory cortex as well as in the anterior cingulate cortex, a region responsible for emotional learning and for encoding the affective "aversiveness" to nociceptor stimulation (Johansen et al., 2001), although cortical responsiveness to acute noxious stimulation was not affected. These data suggest that GluR-A-containing AMPA receptors could contribute to pain-related plasticity in cortical regions involved in the perception, memory, and emotional modulation of pain and provide a basis for testing these hypotheses in region-specific, conditional GluR-deficient mice.

In summary, the present study demonstrates that AMPA receptors are important determinants of pathological nociceptive sensitivity and suggests their potential relevance in therapeutic approaches toward the prevention and treatment of chronic inflammatory pain.

Experimental Procedures

Knockout Mice

Null mutant mice were created by targeted removal of exon 11 from GluR-A (*GRIA1*), GluR-C (*GRIA3*), and the GluR-B (*GRIA2*) genes, respectively, as described previously (Zamanillo et al., 1999; Borchardt, 2002; Shimshek et al., submitted). *GluR-A*$^{-/-}$ mice and *GluR-C*$^{-/-}$ mice were crossed back into the C57BL6 strain, and the *GluR-B*$^{-/-}$ mice were crossed back into the CD1 strain, each for more than eight generations. GluR gene knockout mice and control littermates were obtained by interbreading heterozygous GluR gene knockout mice.

Immunohistochemistry

The following antibodies were used: rabbit polyclonal anti-substance P antiserum, rabbit polyclonal anti-GluR-B and anti-GluR-A antisera (Chemicon International, Hofheim, Germany); rabbit polyclonal anti-Fos antibody (Merck Biosciences GmbH, Germany); rabbit anti-phospho-p44/42 Map Kinase (Thr202/Tyr204) antibody (Cell Signaling Technology, Germany); and polyclonal rabbit anti-ERK-1 and anti-ERK-2 antisera (Santa Cruz Biotechnology, Heidelberg, Germany). Mice were perfused with 4% paraformaldehyde (PFA) and spinal cords, brains, or dorsal root ganglia were extracted and postfixed overnight in 4% PFA. Immunohistochemistry was performed on vibratome sections (50 μm) or cryosections (20 μm) using standard reagents and protocols (Vector Laboratories, Burlingame). Sections from treatment groups to be compared were stained and photographed together, and care was taken to ensure that the staining reaction was within the linear range. Brightfield images were taken under similar illumination conditions. In some experiments, staining intensity per unit area was measured densitometrically (Scion Image software) over selected areas using unstained areas in the ventral horn or the intermediate zone between the dorsal and ventral horns in the same section for subtraction of background staining. The values of background staining (but not white matter staining) were found to be very consistent across different sections within one staining experiment and were subtracted from staining intensities over areas of interest. Data was averaged from at least four areas/section and at least three sections/mouse. TRITC-conjugated streptavidin (Vector Laboratories) was used to detect biotinyl-

ated Isolectin-B4 and visualized using a laser-scanning confocal microscope TCS-AOBS (Leica, Bensheim, Germany).

Cobalt Uptake in Mouse Spinal Cord Slices

We used kainate-induced cobalt uptake as a functional marker for cells expressing Ca^{2+}-permeable AMPA receptors (Engelman et al., 1999). Lumbar spinal cord was rapidly removed from *GluR-A*$^{-/-}$ and *GluR-B*$^{-/-}$ mice and their corresponding wild-type littermates under ether anesthesia and sliced at 400 μm on a vibratome in 95% CO_2/5% O_2-bubbled Kreb's buffer, treated with 250 μm kainic acid (Sigma) and 1.5 mM cobalt chloride in Kreb's buffer containing 0.5 μm tetrodotoxin (Sigma) and D-amino-phosphonopentanoic acid (D-APV, 100 μM; Tocris, Germany) at room temperature for 20 min and processed for cobalt histochemistry with ammonium sulphide. Slices were fixed overnight with 4% PFA in PBS, immersed in sucrose, cryosectioned at 20 μm, and subjected to silver intensification. All cobalt-positive cells were counted in specified spinal laminae, and the mean number per lamina was estimated from at least six slices per genotype.

Spinal Cord Slice Preparation and Electrophysiological Recordings

Transverse slices (250 μm thick) of the lumbar spinal cord were prepared from 8- to 14-day-old mice of both sexes as described previously (Ahmadi et al., 2002). Whole-cell patch-clamp recordings were performed from neurons located in spinal lamina II, which were visually identified using the infrared gradient contrast technique coupled to a video microscopy system (Dodt and Zieglgänsberger, 1994). Slices were continuously superfused with external solution, which contained 125 mM NaCl, 26 mM $NaHCO_3$, 1.25 mM NaH_2PO_4, 2.5 mM KCl, 2 mM $CaCl_2$, 1 mM $MgCl_2$, 10 mM glucose (pH 7.30, 315 mosmol/l) and was bubbled with 95% O_2, 5% CO_2. Patch pipettes (4–5 MΩ) were filled with internal solution containing 130 mM K-gluconate, 20 mM KCl, 2 mM $MgCl_2$, 0.05 mM EGTA, 3 mM Na-ATP, 0.1 mM Na-GTP, 10 mM Na-HEPES (pH 7.30). QX-314 (5 mM) was added to the internal solution to block voltage-activated sodium currents. Postsynaptic current responses (PSCs) were elicited at a frequency of 1/15 s by extracellular electrical stimulation (100 μs, 3–10 V) using a glass electrode filled with standard extracellular solution and placed about 50 μm from the recorded neuron. Excitatory AMPA or NMDA receptor-mediated PSCs (AMPA EPSCs and NMDA EPSCs) were recorded at room temperature in the continuous presence of strychnine (0.3 μM) and bicuculline (10 μM), which were used to block glycine and $GABA_A$ receptor-mediated inhibitory PSCs. AMPA EPSCs were recorded at a holding potential of −80 mV. NMDA EPSCs were recorded at +40 mV to relieve the Mg^{2+} block and in the additional presence of the AMPA receptor antagonist NBQX (10 μM). Short hyperpolarizing voltage steps to −90 mV were applied every minute to monitor input and access resistance.

VRP and Wind-Up Recordings

Hemisected preparations of spinal cords from neonatal mice (P5–P9) of both sexes were used to record spinal cord reflexes as described previously (Heppenstall and Lewin, 2001). The L4–L5 dorsal root was stimulated via a glass suction electrode at currents sufficient to activate C- and A-fibers (500 μA, 500 μs). The A-fiber-mediated component of the VRP was measured as the maximal response to dorsal root stimulation, and C-fiber responses were measured as the response 2 s after stimulation and as the integrated area of the VRP. Wind-up was evoked by repetitive stimulation at 1 Hz for 20 s and was determined by normalizing the increase in size of the VRP to the initial magnitude and expressing it as a percentage increase. Traces were acquired with the Powerlab 4.0 system using SUPERSCOPE software (ADInstruments GmbH, Spechbach, Germany).

Dorsal Root Stimulation in Spinal Cord Slices

The lumbosacral segment (L1–S1) of adult spinal cord was removed with intact dorsal roots attached and was placed in cold (0°C–4°C) Krebs solution, consisting of 127 mM NaCl; 1.8 mM KCl; 2.4 mM $CaCl_2$; 1.3 mM $MgSO_4$; 1.2 mM KH_2PO_4; 26 mM $NaHCO_3$; 15 mM Glucose, and preequilibrated with carbogen (95% O_2 and 5% CO_2). Spinal cord slices (400–600 μm) with at least one dorsal root attached were prepared, and the dorsal root was stimulated with a suction electrode at C-fiber intensity. Electrical stimulation was done at 100 Hz (high frequency), 1 s duration each for five times at 10 s intervals or at 900 pulses at 1 Hz (low frequency). Thirty minutes after stimulation, the tissue was fixed with 4% PFA overnight and then processed for immunohistochemistry with anti-pERK/ERK-1/ERK-2. Control slices were treated the same way as the stimulated slices, with dorsal roots placed in suction electrodes, but were not stimulated. To estimate the rostrocaudal distance over which ERK phosphorylation occurs following dorsal root stimulation, pERK immunoreactivity was estimated densitometrically (above) in serial sections at every 40 μm along the rostrocaudal axis from the point of root entry.

Behavioral Analysis in Mice

All animal experimental protocols were approved by the local governing committee. All behavioral measurements were done in awake, unrestrained, age-matched adult (more than 3 months old) mice of both sexes. Mice were acclimatized to the experimental set ups several times before the analysis. In all experiments, the experimentor was blinded to the genotypes of the mice being analyzed.

Plantar Test and Paw Inflammation

Determination of latency of paw withdrawal in response to noxious heat and graded pressure was done using the plantar test apparatus (Hargreaves et al., 1988; Ugo Basile, Italy) with a sensitivity of 0.1 s (Kolhekar et al., 1997) ($n = 7–14$ per group). Nociceptive thresholds and the dimensions of the each hindpaw were recorded before and at defined intervals after intraplantar injection of CFA (20 μl). Dimensions of the hindpaw were measured using a fine calliper and by plethysmometry. Paw edema was calculated as a change in paw volume (length × breadth × height) as well as using a pleythsmometer (Ugo Basile, Italy) as described in details by Cirino et al. (1989).

Tail Flick Reflex

The nociceptive tail flick reflex was evoked by noxious heat applied via an infrared light source (Ugo Basile, Italy) with a sensitivity of 0.1 s as described previously (Kolhekar et al., 1993).

Formalin Test and Capsaicin Test

Formalin (1%, 20 μl) or capsaicin (0.06%, 10 μl) was injected into the plantar surface of the right hindpaw and the duration of nocifensive behaviors, including lifting, licking, or flinching of the injected paw, was measured for 5 min after capsaicin injection or in 5 min bins for 50 min after formalin injection as described previously (Laird et al., 2001; Tjolsen et al., 1992).

Data Analysis and Statistics

All data are presented as mean ± SEM. Student's t tests or the analysis of variance (ANOVA) for random measures followed by post hoc Fisher's LSD tests were utilized to determine statistically significant differences ($p \leq 0.05$).

Acknowledgments

The authors are grateful to Derya Shimshek for help with genotyping of GluR mutant mice; to Hans-Joseph Wrede for technical assistance; and to G.F. Gebhart, Stefan Offermanns, and Thomas Kuner for critically reading an earlier version of the manuscript. This work was supported by an Emmy Noether grant from the Deutsche Forschungsgemeinschaft (DFG) to R.K., DFG grants to H.U.Z., and by the Max-Planck Society (R.S. and P.H.S.).

Received: May 11, 2004
Revised: October 13, 2004
Accepted: October 14, 2004
Published: November 17, 2004

References

Ahmadi, S., Lippross, S., Neuhuber, W.L., and Zeilhofer, H.U. (2002). PGE_2 selectively blocks inhibitory glycinergic neurotransmission onto rat superficial dorsal horn neurons. Nat. Neurosci. *5*, 34–40.

Albuquerque, C., Lee, C.J., Jackson, A.C., and MacDermott, A.B. (1999). Subpopulations of GABAergic and non-GABAergic rat dorsal

horn neurons express Ca2+-permeable AMPA receptors. Eur. J. Neurosci. *11*, 2758–2766.

Borchardt, T. (2002). Die Konstruktion von Mäusen mit veränderten AMPA-Rezeptoren. Dissertation, University of Heidelberg, Germany.

Brown, K.M., Wrathall, J.R., Yasuda, R.P., and Wolfe, B.B. (2002). Quantitative measurement of glutamate receptor subunit protein expression in the postnatal rat spinal cord. Brain Res. Dev. Brain Res. *137*, 127–133.

Burnashev, N., Monyer, H., Seeburg, P.H., and Sakmann, B. (1992). Divalent ion permeability of AMPA receptor channels is dominated by the edited form of a single subunit. Neuron *8*, 189–198.

Cirino, G., Peers, S.H., Wallace, J.L., and Flower, R.J. (1989). A study of phospholipase A2-induced oedema in rat paw. Eur. J. Pharmacol. *166*, 505–510.

Davies, J., and Watkins, J.C. (1983). Role of excitatory amino acid receptors in mono- and polysynaptic excitation in the cat spinal cord. Exp. Brain Res. *49*, 280–290.

Dodt, H.U., and Zieglgänsberger, W. (1994). Infrared videomicroscopy: a new look at neuronal structure and function. Trends Neurosci. *17*, 453–458.

Engelman, H.S., and MacDermott, A.B. (2004). Presynaptic ionotropic receptors and control of transmitter release. Nat. Rev. Neurosci. *5*, 135–145.

Engelman, H.S., Allen, T.B., and MacDermott, A.B. (1999). The distribution of neurons expressing calcium-permeable AMPA receptors in the superficial laminae of the spinal cord dorsal horn. J. Neurosci. *19*, 2081–2089.

Fang, L., Wu, J., Lin, Q., and Willis, W.D. (2003a). Protein kinases regulate the phosphorylation of the GluR1 subunit of AMPA receptors of spinal cord in rats following noxious stimulation. Brain Res. Mol. Brain Res. *118*, 160–165.

Fang, L., Wu, J., Zhang, X., Lin, Q., and Willis, W.D. (2003b). Increased phosphorylation of the GluR1 subunit of spinal cord alpha-amino-3-hydroxy-5-methyl-4-isoxazole propionate receptor in rats following intradermal injection of capsaicin. Neuroscience *122*, 237–245.

Flor, H. (2000). The functional organization of the brain in chronic pain. Prog. Brain Res. *129*, 313–322.

Flor, H. (2002). Painful memories. Can we train chronic pain patients to 'forget' their pain? EMBO Rep. *3*, 288–291.

Gebhart, G.F. (2004). Descending modulation of pain. Neurosci. Biobehav. Rev. *27*, 729–737.

Geiger, J.R., Melcher, T., Koh, D.S., Sakmann, B., Seeburg, P.H., Jonas, P., and Monyer, H. (1995). Relative abundance of subunit mRNAs determines gating and Ca2+ permeability of AMPA receptors in principal neurons and interneurons in rat CNS. Neuron *15*, 193–204.

Gu, J.G., Albuquerque, C., Lee, C.J., and MacDermott, A.B. (1996). Synaptic strengthening through activation of Ca2+-permeable AMPA receptors. Nature *381*, 793–796.

Hargreaves, K.M., Dubner, F., Brown, F., Flores, C., and Joris, J. (1988). A new and sensitive method for measuring thermal nociception in cutaneous hyperalgesia. Pain *32*, 77–88.

Heppenstall, P.A., and Lewin, G.R. (2001). BDNF but not NT-4 is required for normal flexion reflex plasticity and function. Proc. Natl. Acad. Sci. USA *98*, 8107–8112.

Ikeda, H., Heinke, B., Ruscheweyh, R., and Sandkuhler, J. (2003). Synaptic plasticity in spinal lamina I projection neurons that mediate hyperalgesia. Science *299*, 1237–1240.

Ji, R.R., Baba, H., Brenner, G.J., and Woolf, C.J. (1999). Nociceptive-specific activation of ERK in spinal neurons contributes to pain hypersensitivity. Nat. Neurosci. *2*, 1114–1119.

Ji, R.R., Befort, K., Brenner, G.J., and Woolf, C.J. (2002). ERK MAP kinase activation in superficial spinal cord neurons induces prodynorphin and NK-1 upregulation and contributes to persistent inflammatory pain hypersensitivity. J. Neurosci. *22*, 478–485.

Jia, Z., Agopyan, N., Miu, P., Xiong, Z., Henderson, J., Gerlai, R., Taverna, F.A., Velumian, A., MacDonald, J., Carlen, P., et al. (1996). Enhanced LTP in mice deficient in the AMPA receptor GluR2. Neuron *17*, 945–956.

Johansen, J.P., Fields, H.L., and Manning, B.H. (2001). The affective component of pain in rodents: direct evidence for a contribution of the anterior cingulate cortex. Proc. Natl. Acad. Sci. USA *98*, 8077–8082.

Ju, W., Morishita, W., Tsui, J., Gaietta, G., Deerinck, T.J., Adams, S.R., Garner, C.C., Tsien, R.Y., Ellisman, M.H., and Malenka, R.C. (2004). Activity-dependent regulation of dendritic synthesis and trafficking of AMPA receptors. Nat. Neurosci. *7*, 244–253.

Kawahara, Y., Ito, K., Sun, H., Aizawa, H., Kanazawa, I., and Kwak, S. (2004). Glutamate receptors: RNA editing and death of motor neurons. Nature *427*, 801.

Kolhekar, R., Meller, S.T., and Gebhart, G.F. (1993). Characterisation of the role of spinal NMDA receptors in thermal nociception in the rat. Neuroscience *57*, 385–395.

Kolhekar, R., Murphy, S., and Gebhart, G.F. (1997). Thalamic NMDA receptors modulate inflammation-produced hyperalgesia in the rat. Pain *71*, 31–40.

Laird, J.M.A., Roza, C., De Felipe, C., Hunt, S.P., and Cervero, F. (2001). Role of central and peripheral tachykinin NK1 receptors in capsaicin-induced pain and hyperalgesia in mice. Pain *90*, 97–103.

Lee, C.J., Bardoni, R., Tong, C.K., Engelman, H.S., Joseph, D.J., Magherini, P.C., and MacDermott, A.B. (2002). Functional expression of AMPA receptors on central terminals of rat dorsal root ganglion neurons and presynaptic inhibition of glutamate release. Neuron *35*, 135–146.

Lee, H.K., Takamiya, K., Han, J.S., Man, H., Kim, C.H., Rumbaugh, G., Yu, S., Ding, L., He, C., Petralia, R.S., et al. (2003). Phosphorylation of the AMPA receptor GluR1 subunit is required for synaptic plasticity and retention of spatial memory. Cell *112*, 631–643.

Li, J., Simone, D.A., and Larson, A.A. (1999). Windup leads to characteristics of central sensitization. Pain *79*, 75–82.

Liu, S.-Q.J., and Cull-Candy, S. (2000). Synaptic activity at calcium-permeable AMPA receptors induces a switch in receptor subtype. Nature *405*, 454–458.

Lu, C.R., Hwang, S.J., Phend, K.D., Rustioni, A., and Valtschanoff, J.G. (2002). Primary afferent terminals in spinal cord express presynaptic AMPA receptors. J. Neurosci. *22*, 9522–9529.

Ma, Q.P., and Woolf, C.J. (1996). Basal and touch-evoked fos-like immunoreactivity during experimental inflammation in the rat. Pain *67*, 307–316.

Malinow, R., and Malenka, R.C. (2002). AMPA receptor trafficking and synaptic plasticity. Annu. Rev. Neurosci. *25*, 103–126.

Monyer, H., Seeburg, P.H., and Wisden, W. (1991). Glutamate-operated channels: developmentally early and mature forms arise by alternative splicing. Neuron *6*, 799–810.

Nagy, J.I., and Hunt, S.P. (1982). Fluoride-resistant acid phosphatase-containing neurones in dorsal root ganglia are separate from those containing substance P or somatostatin. Neuroscience *7*, 89–97.

Nagy, G.G., Al-Ayyan, M., Andrew, D., Fukaya, M., Watanabe M., and Todd, A.J. (2004). Widespread expression of the AMPA receptor GluR2 subunit at glutamatergic synapses in the rat spinal cord and phosphorylation of GluR1 in response to noxious stimulation revealed with an antigen-unmasking method. J. Neurosci. *24*, 5766–5777.

Petralia, R.S., Wang, Y.-X., Mayat, E., and Wenthold, R.J. (1997). Glutamate receptor subunit 2-selective antibody shows a differential distribution of Ca^{2+}-impermeable AMPA receptors among populations of neurons. J. Comp. Neurol. *385*, 456–476.

Reisel, D., Bannerman, D.M., Schmitt, W.B., Deacon, R.M., Flint, J., Borchardt, T., Seeburg, P.H., and Rawlins, J.N. (2002). Spatial memory dissociations in mice lacking GluR1. Nat. Neurosci. *5*, 868–873.

Sandkühler, J. (2000). Learning and memory in pain pathways. Pain *88*, 113–118.

Sandkühler, J. (2002). Fear the pain. Lancet *360*, 426.

Seeburg, P.H., Single, F., Kuner, T., Higuchi, M., and Sprengel, R.

(2001). Genetic manipulation of key determinants of ion flow in glutamate receptor channels in the mouse. Brain Res. *13*, *907*, 233–243.

Shi, S., Hayashi, Y., Esteban, J.A., and Malinow, R. (2001). Subunit-specific rules governing AMPA receptor trafficking to synapses in hippocampal pyramidal neurons. Cell *105*, 331–343.

Sutton, M.A., Schmidt, E.F., Choi, K.H., Schad, C.A., Whisler, K., Simmons, D., Karanian, D.A., Monteggia, L.M., Neve, R.L., and Self, D.W. (2003). Extinction-induced upregulation in AMPA receptors reduces cocaine-seeking behaviour. Nature *421*, 70–75.

Takahashi, T., Svoboda, K., and Malinow, R. (2003). Experience strengthening transmission by driving AMPA receptors into synapses. Science *299*, 1585–1588.

Thomas, G.M., and Huganir, R.L. (2004). MAPK cascade signalling and synaptic plasticity. Nat. Rev. Neurosci. *5*, 173–183.

Thomas, M.J., Beurrier, C., Bonci, A., and Malenka, R.C. (2001). Long-term depression in the nucleus accumbens: a neural correlate of behavioral sensitization to cocaine. Nat. Neurosci. *4*, 1217–1223.

Tinazzi, M., Fiaschi, A., Rosso, T., Faccioli, F., Grosslercher, J., and Aglioti, S.M. (2000). Neuroplastic changes related to pain occur at multiple levels of the human somatosensory system: A somatosensory-evoked potentials study in patients with cervical radicular pain. J. Neurosci. *20*, 9277–9283.

Tjolsen, A., Berge, O.G., Hunskaar, S., Rosland, J.H., and Hole, K. (1992). The formalin test: an evaluation of the method. Pain *51*, 5–17.

Tolle, T.R., Berthele, A., Zieglgänsberger, W., Seeburg, P.H., and Wisden, W. (1993). The differential expression of 16 NMDA and non-NMDA receptor subunits in the rat spinal cord and in periaqueductal gray. J. Neurosci. *13*, 5009–5028.

Vaccarino, A.L., and Melzack, R. (1992). Temporal processes of formalin pain: differential role of the cingulum bundle, fornix pathway and medial bulboreticular formation. Pain *49*, 257–271.

Wilding, T.J., and Huettner, J.E. (1995). Differential antagonism of alpha-amino-3-hydroxy-5-methyl-4-isoxazolepropionic acid-preferring and kainate-preferring receptors by 2,3-benzodiazepines. Mol. Pharmacol. *47*, 582–587.

Willis, W.D., Jr. (1997). Is central sensitization of nociceptive transmission in the spinal cord a variety of long-term potentiation? Neuroreport. *8*, iii.

Woolf, C.J., and Salter, M.W. (2000). Neuronal plasticity: increasing the gain in pain. Science *288*, 1765–1769.

Zamanillo, D., Sprengel, R., Hvalby, O., Jensen, V., Burnashev, N., Rozov, A., Kaiser, K.M., Koster, H.J., Borchardt, T., Worley, P. et al. (1999). Importance of AMPA receptors for hippocampal synaptic plasticity but not for spatial learning. Science *284*, 1805–1811.

Zhou, Q.Q., Imbe, H., Zou, S., Dubner, R., and Ren, K. (2001). Selective upregulation of the flip-flop splice variants of AMPA receptor subunits in the rat spinal cord after hindpaw inflammation. Brain Res. Mol. Brain Res. *88*, 186–193.